

## Supporting Information

### Stop-Flow Lithography for the Production of Shape-Evolving Degradable Microgel Particles

Dae Kun Hwang<sup>1</sup>, John Oakey<sup>2</sup>, Mehmet Toner<sup>2</sup>, Jeffrey A. Arthur<sup>3</sup>, Kristi S. Anseth<sup>3</sup>, Sunyoung Lee<sup>4</sup>, Adam Zeiger<sup>4</sup>, Krystyn J. Van Vliet<sup>4</sup>, Patrick S. Doyle<sup>1,\*</sup>

<sup>1</sup>Department of Chemical Engineering,  
Massachusetts Institute of Technology  
Cambridge, Massachusetts, 02139

<sup>2</sup>BioMEMS Resource Center and Center for Engineering in Medicine  
Harvard Medical School and Massachusetts General Hospital  
Charlestown, MA 02129

<sup>3</sup>Department of Chemical and Biological Engineering  
University of Colorado, Boulder  
Boulder, CO 80403

<sup>4</sup>Department of Materials Science and Engineering  
Massachusetts Institute of Technology  
Cambridge, Massachusetts, 02139

\* Corresponding author (pdoyle@mit.edu)

**Contents:** Materials and Methods  
Figure S1  
Figure S2

## Materials and Methods

### *Materials*

The acrylated biodegradable macromer (see Figure. 1a), poly(lactic acid)-*b*-poly(ethylene glycol)-*b*-poly(lactic acid) diacrylate, (A-PLA-*b*-PEG-*b*-PLA-A), was synthesized according to the method originally reported by Sawheny, *et al.*,<sup>1</sup> Briefly, a two-step process was used to synthesize the macromers. First, the dihydroxy PEG was reacted with D,L-lactide at 135°C for 6h under argon with stannous octoate as a catalyst. The resulting intermediate block copolymer was then prepared via dissolving in methylene chloride and precipitating in diethyl ether, and by further vacuum filtering and drying under vacuum. Second, the chain ends of the copolymer were acrylated after dissolving the polymer in methylene chloride with triethylamine and acryloyl chloride. The solution was reacted under argon at 0°C and was further reacted at room temperature. Finally, a fluffy white powder was obtained by a second precipitation in diethyl ether followed by vacuum filtration. The macromer, diacrylate PLA-*b*-PEG-*b*-PLA, used in this study consists of a 4600 molecular weight (MW) PEG chain with an average of 9.5 repeating lactide units on each side. Acrylate groups functionalized on both ends of the chain (95% yield) allow formation of a cross-linked network via photopolymerization. Chemicals used in the macromer synthesis are: PEG (4600 MW, Adrich), DL-lactide (Polysciences), triethylamine (Aldrich), acryloyl chloride (Aldrich), diethyl ether (Fisher), and stannous octanote (Aldrich).

Macromer solutions containing the diacrylate PLA-*b*-PEG-*b*-PLA at three different concentrations, 10, 20, and 30 % (w/w) were prepared by dissolving them in ethanol/distilled water with 4% (w/w) 2-hydroxy-1-(4-(hydroxyethoxy)phenyl)-2methyl-1propanone (Irgacure-2959, Aldrich) and 0.5 % (w/w) n-vinylpyrrolidone (NVP, Aldrich). A 30% (w/w) poly(ethylene glycol) diacrylate (PEGDA 4000 MW, Polyscience) solution in ethanol/distilled water served as the control was also prepared with 4% Irgacure-2959 and 0.5% NVP. For the fluorescent visualization, methacryloxyethyl thiocarbamoyl Rhodamine B (Polysciences) or green fluorescent microbeads (carboxylated solid-latex polystyrene spheres, 2µm DA, Polysciences) were added to the prepolymer solutions.

### *Microfluidic device and UV-polymerization scheme*

Microfluidic channels were fabricated by soft lithography. Briefly, polydimethylsiloxane (PDMS, Sylgard 184, Dow Corning) was poured upon an SU-8 photoresist (Microchem Corp.)<sup>2</sup> patterned

silicon wafer and cured to create a bas-relief microchannel network. For all experiments, we used straight rectangular cross-section channels with height,  $h = 30 \mu\text{m}$  and width,  $w = 300 \mu\text{m}$ . The channels together with outlet reservoirs were cut out from the wafer with a scalpel and an inlet port was punched into the device with a blunt syringe (Small Parts, Inc.) to introduce the prepolymer solutions. PDMS channels (Figure 1a) were assembled by sealing the channels to PDMS-coated glass slides. The assembled devices were mounted on an inverted microscope (Axiovert 200, Zeiss). The prepolymer solutions were then introduced into the PDMS devices by air pressure. An automated-pressure valve system<sup>3</sup> was used to flow and stop the solutions.

Photomasks featured with a triangle shape for the diacrylate PLA-*b*-PEG-*b*-PLA solutions and rectangle for the PEGDA were designed using AUTOCAD and printed with 20000 dpi at CAD Art Services (Poway, California). The masks were placed in the field-stop of the microscope and the designed features (triangle and rectangles) were projected to the solutions by exposing wide excitation ultraviolet (UV) filter set (11000v2: UV, Chroma) from a 100 W HB mercury lamp when the flow of the solutions was completely stopped. Desired pulses of UV excitations were obtained by a computer-aided UV shutter system (UniBlitz). Incident UV intensities were measured using a UVA Power and Dose meter (ACCU-CAL-30 UVA, DYMAX). In our entire experiments, we fixed UV exposure time constant (800 msec) and varied UV intensity to study effect of UV dose on size and erosion behavior of hydrogel particles.

#### *Particle recovery and incubation*

Particles collected in a reservoir after photopolymerization were transferred into a microcentrifuge tube and then rinsed several times using a pH 7.2 phosphate buffered solution (PBS, Invitrogen) with 50 % ethanol and 0.25 % Tween 20 to remove all residual of unreacted oligomers and fluorescent molecules. The particles were then additionally rinsed several times only using the PBS with 0.5% Tween 20 until all ethanol was gone and suspended in that PBS for degradation studies.

Degradation of the polymerized hydrogels, suspended in the PBS, was observed in a PDMS reservoir, which was placed in an insulated water bath and maintained at 37°C. In order to allow visual observation under the microscope and to avoid evaporation of the bulk, the reservoir was built on a thin glass layer in such a way that an inner reservoir containing hydrogel particles was immersed in the PBS in an outer reservoir. The reservoir was fabricated by sealing two

different sizes of PDMS rectangular frames ( $\sim 20 \times 20 \times 8 \text{ mm}^3$  and  $\sim 7 \times 7 \times 4 \text{ mm}^3$ ) on a thin glass layer. The inner PDMS frame was positioned in the center of the outer frame, and was first filled with hydrogel particles suspended in the PBS, and capped with a thin layer of PDMS. Then, the outer PDMS reservoir was filled with the PBS and again capped with a thin layer of PDMS. The reservoir was finally placed in the water bath and maintained at  $37^\circ\text{C}$ .

### *Image analysis*

Formations of hydrogel particles were visualized using a CCD camera (KPM1A, Hitachi) mounted on the microscope, and for the fluorescent visualization, the resulting particles were visualized using an orange long pass filter set (XF 101-2, Omega) for Rhodamine B and a green filter set (XF 100-2, Omega) for the microbeads. Captured optical images were processed using NIH Image software. A Nikon D200 camera (Digital SLR) was also used to capture florescent and bright-field color images of hydrogel particles. For degradation excursions, at specific time points, PDMS reservoirs containing the hydrogel particles incorporated with Rhodamine B were removed from the water bath, and their fluorescent images were captured and analyzed using the Image J software package.

### *Atomic force microscopy-enabled nanoindentation*

An atomic force microscope (AFM, Agilent Technology) was incorporated within an optical microscope (IX 81, Olympus) to enable facile positioning of AFM cantilevers above individual particles (See Figure 3c). Calibration of AFM  $\text{Si}_3\text{N}_4$  cantilevers of nominal spring constant  $k = 0.1 \text{ N/m}$  and probe radius  $R = 25 \text{ nm}$  (Veeco) was conducted as described previously.<sup>4-6</sup> Briefly, inverse optical lever sensitivity [ $\text{nm/V}$ ] (InvOLS) was measured from deflection-displacement curves recorded on rigid glass substrates. Spring constants [ $\text{nN/nm}$ ] of AFM cantilevers were measured via thermal activation recording of deflection and the Fourier Transform (FFT) of cantilever amplitude as a function of oscillation frequency fitted with simple harmonic oscillation function. For each particle composition and degradation time point, at least 30 replicate indentations were acquired, and the elastic response analyzed to maximum depths of  $20 \text{ nm}$  (See Figure S2). Microhydrogel particles were indented in the fully immersed state in phosphate buffered saline (PBS), and stored at room temperature between observation intervals. Acquired probe deflection-displacement responses were converted offline (Scanning Probe Imaging

Processor, Image Metrology), using measured spring constants and InvOLS, to force-depth responses. Elastic moduli  $E$  were calculated by applying a modified Hertzian model of spherical contact to the loading segment of the force-depth response, as detailed elsewhere<sup>6,7</sup> with the scientific computing software Igor Pro (Wavemetrics). Computed elastic moduli  $E$  are reported as average  $\pm$  standard deviation, and all statistical analyses were conducted with one-way ANOVA (Tukey analysis).

### Figure S1 and Figure S2

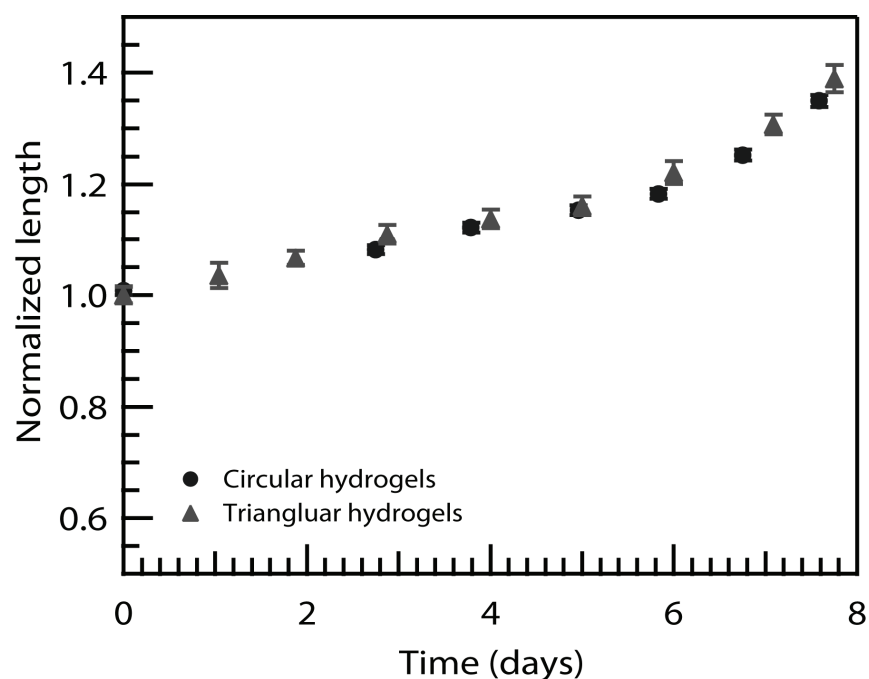


**Figure S1.** Swelling behavior of degradable hydrogel particles (PLA-*b*-PEG-*b*-PLA 20 wt%) with two different shapes (disks with a diameter 130  $\mu\text{m}$  and triangles with a side length 61  $\mu\text{m}$  on Day 0). Applied UV dose is 0.096  $\text{J}/\text{cm}^2$ . The triangular hydrogels correspond to those in Figure 4b.

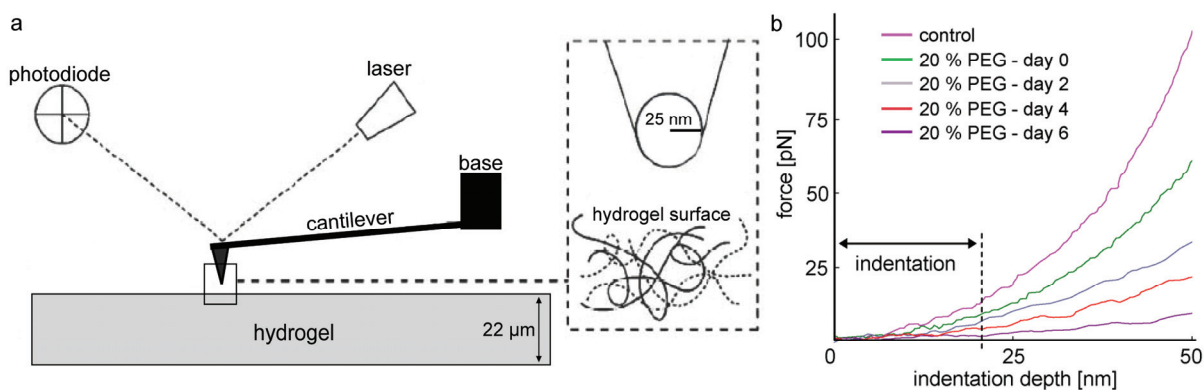


**Figure S2.** (a) Schematic of AFM indentation and (b) nanoindentation force-depth responses for non-degradable (control, rectangles, PEGDA 30 wt %) and degradable hydrogels (triangles, diacrylate PLA-*b*-PEG-*b*-PLA 20 wt %). To determine elastic moduli from these force-depth data, indentation responses were analyzed over the depth range for which a spherical elastic response is valid (<20 nm), as indicated by the vertical dashed line. Hydrogel thicknesses are ~ 26 μm (control, rectangles) and ~ 22 μm (triangles, diacrylate PLA-*b*-PEG-*b*-PLA 20 wt %).

Elastic moduli  $E$  were calculated from the force-depth indentation responses acquired via atomic force microscopy (AFM)-enabled indentation within a fluid cell, allowing full immersion of the hydrogel microparticles in phosphate buffered saline at room temperature (Figure S2a). These particles were supported by rigid glass slides to which they nonspecifically adhered and remained stationary during each indentation experiment. Cantilevered conospherical probes of radius  $R = 25$  nm and nominal spring constant  $k = 0.1$  N/m were deflected against the hydrogel particle surface, and the deflection of the cantilever free-end during piezo-actuated displacement of the cantilever base was recorded via a laser photodiode-piezoactuation feedback loop. Conversion of the raw signals to force-depth responses were obtained as follows. Cantilever free-end deflection reported by the photodiode in units of [V] was converted to force [nN] via multiplication of this deflection by the inverse optical lever sensitivity or InvOLS [nm/V] and by the actual spring constant  $k$  of the cantilever [nN/nm]; spring constants were measured through the thermal oscillation method described in the text and Supplementary Reference 6. Cantilever base displacement [nm] was converted to indentation depth [nm] as the difference between the cantilever base displacement and cantilever free-end deflection.

Representative force-depth responses for the control and 20 wt% PEG particles over degradation times are shown in Figure S2b. Qualitatively, these data show that the 20 wt% PEG particle response becomes increasingly compliant with increasing degradation time (the curves

shift downward with degradation time). Quantitatively, elastic moduli  $E$  were calculated by fitting the loading responses (Figure S2b) to the Hertzian model of spherical elastic contact<sup>8</sup> as detailed elsewhere.<sup>6,7</sup> This contact model relates the force  $P$  to the indentation depth  $h$  through the material elastic modulus  $E$  and indenter radius  $R$  as:  $P = \frac{4}{3}ER^{1/2}h^{3/2}$ . The initial contact point for each force-depth response was identified as the point at which the log(force) vs. log(depth) curve transitioned to from a line of approximately zero slope to a line of slope approximately 3/2, according to this Hertzian power law.<sup>8,9</sup> To maximize the applicability of this spherical-contact elastic model (given that  $R = 25$  nm for this conospherical probe) and to minimize any mechanical contributions from the underlying glass support, the force-depth responses were analyzed to depths of 20 nm, as indicated in Figure S2b.

## References

- (1) Sawhney, A. S.; Pathak, C. P.; Hubbell, J. A. *Macromolecules* **2001**, *26*, 581.
- (2) Duffy, D. C.; McDonald, J. C.; Schueller, O. J. A.; Whitesides, G. M. *Anal. Chem.* **1998**, *70*, 4974-4984.
- (3) Dendukuri, D.; Gu, S. S.; Pregibon, D. C.; Hatton, T. A.; Doyle, P. S. *Lab Chip* **2007**, *7*, 818-828.
- (4) Butt, H. J.; Jaschke, M. *Nanotechnology* **1995**, *6*, 1-7.
- (5) Hutter, J. L.; Bechhoefer, J. *Rev. Sci. Instrum.* **1993**, *64*, 1868-1873.
- (6) Thompson, M. T.; Berg, M. C.; Tobias, I. S.; Rubner, M. F.; Van Vliet, K. J. *Biomaterials* **2005**, *26*, 6836-6845.
- (7) Thompson, M. T.; Berg, M. C.; Tobias, I. S.; Lichter, J. A.; Rubner, M. F.; Van Vliet, K. J. *Biomacromolecules* **2006**, *7*, 1990-1995.
- (8) Hertz, H *Verhandlungen des Vereins zur Beförderung des Gewerbefleisses* **1882**, 90
- (9) Guo, S.; Hong, L.; Akhremitchev, B. B.; Simon, J. D. *Photochemistry and Photobiology* **2008**, *84*, 671-678.